



## DOM Molecular Weight Fractionation and Fluorescence Quantum Yield Assessment Using a Coupled In-Line SEC Optical Property System

Hanson, Blair; Wünsch, Urban; Buckley, Shelby; Fischer, Sarah; Leresche, Frank; Murphy, Kathleen; D'Andrilli, Juliana; Rosario-Ortiz, Fernando L.

*Published in:*  
ACS EST Water

*Link to article, DOI:*  
[10.1021/acsestwater.2c00318](https://doi.org/10.1021/acsestwater.2c00318)

*Publication date:*  
2022

*Document Version*  
Peer reviewed version

[Link back to DTU Orbit](#)

*Citation (APA):*  
Hanson, B., Wünsch, U., Buckley, S., Fischer, S., Leresche, F., Murphy, K., D'Andrilli, J., & Rosario-Ortiz, F. L. (2022). DOM Molecular Weight Fractionation and Fluorescence Quantum Yield Assessment Using a Coupled In-Line SEC Optical Property System. *ACS EST Water*, 2(12), 2491-2501.  
<https://doi.org/10.1021/acsestwater.2c00318>

---

### General rights

Copyright and moral rights for the publications made accessible in the public portal are retained by the authors and/or other copyright owners and it is a condition of accessing publications that users recognise and abide by the legal requirements associated with these rights.

- Users may download and print one copy of any publication from the public portal for the purpose of private study or research.
- You may not further distribute the material or use it for any profit-making activity or commercial gain
- You may freely distribute the URL identifying the publication in the public portal

If you believe that this document breaches copyright please contact us providing details, and we will remove access to the work immediately and investigate your claim.

# DOM Molecular Weight Fractionation and Fluorescent Quantum Yield Assessment Using a Coupled In-line SEC Optical Property System

Blair Hanson<sup>a,b</sup>, Urban Wünsch<sup>c,d</sup>, Shelby Buckley<sup>a,b</sup>, Sarah Fischer<sup>a,b,f</sup>, Frank Leresche<sup>a,b</sup>, Kathleen Murphy<sup>c</sup>, Juliana D'Andrilli<sup>e</sup>, and Fernando L. Rosario-Ortiz<sup>a,b\*</sup>

<sup>a</sup>Department of Civil, Environmental, and Architectural Engineering  
University of Colorado Boulder, CO 80309, USA

<sup>b</sup>Environmental Engineering Program  
University of Colorado Boulder, CO 80309, USA

<sup>c</sup>Chalmers University of Technology, Department of Architecture and Civil Engineering, Water Environment Technology, SE-41296 Gothenburg

<sup>d</sup>Technical University of Denmark, National Institute of Aquatic Resources, Section for Oceans and Arctic, DK-2800 Kongens Lyngby

<sup>e</sup>Louisiana Universities Marine Consortium, Chauvin, LA 70344, USA

<sup>f</sup>Department of Civil and Environmental Engineering, University of Missouri, Columbia, MO 65201, USA

\*Corresponding author: fernando.rosario@colorado.edu

## ABSTRACT

Size exclusion chromatography (SEC) in combination with optical measurements has become a popular form of analysis to characterize dissolved organic matter (DOM) as a function of molecular size. Here, SEC coupled with in-line absorbance scans and fluorescence emission scans was utilized to derive apparent fluorescence quantum yield ( $\Phi_f$ ) as a function of molecular weight (MW) for DOM. Individual instrument specific SEC-fluorescence detector correction factors were developed by comparison of a SEC based excitation emission matrix (EEM) to an

excitation emission matrix (EEM) generated by a calibrated benchtop fluorometer. The method was then applied to several sample sets to demonstrate how to measure the  $\Phi_f$  of unknown DOM samples and to observe changes to  $\Phi_f$  following a processing mechanism (ozonation). The  $\Phi_f$  of riverine water samples and DOM fulvic acid isolates from Suwannee River and Pony Lake increased from <0.5% to a maximum of ~2.5-3% across the medium to low MW range. Following ozonation of PLFA,  $\Phi_f$  increased most notably in the large MW fractions (elution volumes < 40 mL). Overall, this method provides a means by which highly fluorescent size fractions of DOM can be identified for more detailed analyses of carbon quality and its changes through different processing mechanisms.

#### **Keywords**

Dissolved organic matter; size exclusion chromatography; fluorescence; quantum yield; ozone; optical properties

## SYNOPSIS

A method utilizing size exclusion chromatography with multiple forms of detection is demonstrated to calculate the online fluorescent quantum yield as a function of molecular weight.

## 1. INTRODUCTION

Dissolved organic matter (DOM) is composed of a diverse mixture of compounds originating from the molecular remnants of plants, animal materials, and microbial exudates. DOM represents a major part of the global carbon cycle and is an important factor in numerous chemical and physical processes in natural and engineered systems.<sup>1,2</sup> For example, DOM serves as a substrate for microbial growth and can complex with metals and organic pollutants, impacting their fate in natural waters.<sup>3,4</sup> Additionally, DOM impacts water treatment processes, including reactions with chlorine, resulting in the formation of disinfection byproducts, some of which are harmful to humans if consumed.<sup>5,6</sup> However, due to the complex chemical composition of DOM, determination of its characteristics relies on the development and application of numerous analytical methods.<sup>7</sup>

One property that has received considerable attention in the study of DOM is its average molecular weight and the overall size distribution of sub-components. Although molecular weight (MW) can be assessed using different techniques (e.g., vapor pressure osmometry, field flow fractionation and high resolution mass spectrometry<sup>8-12</sup>), most assessments are based on the use of size exclusion chromatography (SEC).<sup>13-15</sup> SEC can be used to determine the *apparent* MW (AMW) distribution of DOM. Determination of the AMW (in contrast to *absolute* molecular weight) is based on the fact that the separation is not strictly due to molecular weight, but instead based on hydrodynamic size, which is affected by solution chemistry and non-ideal interactions within the SEC-column.<sup>16</sup> Applications of SEC for the study of DOM include systems where

quantification is based on carbon, nitrogen, or optical properties, therefore offering different qualitative and quantitative information about the samples.<sup>13</sup>

The application of fluorescence spectroscopy for the study of DOM has gained significant attention over the past 30 years.<sup>17–20</sup> Three dimensional fluorescence excitation emission matrices (EEMs) are popularly used to distinguish source origin and inform physicochemical properties of DOM.<sup>20–23</sup> While fluorescence offers the possibility to collect signals with high sensitivity and relative simplicity,<sup>24–26</sup> the specific chemical components responsible for DOM fluorescence have yet to be identified.<sup>27</sup> Understanding the chemical characteristics of the main types of fluorophores within DOM would help to address deficiencies in fluorescence analysis, such as spectral overlap between fluorophores and the impacts of local environments on fluorescence signals (see section S-3 in the supplemental information for an expanded discussion on expected chemical groups responsible for absorbance and fluorescence of DOM). Insights into fluorophores highlight fluorescence properties that are sensitive to differences in DOM source and composition and inform how they can be applied, such as the use of DOM fluorescence as a surrogate for wastewater impact.<sup>28</sup>

One fluorescence-based metric, the fluorescence quantum yield ( $\Phi_f$ ), describes the fraction of photons reemitted via fluorescence relative to the number of absorbed photons.<sup>29,30</sup>  $\Phi_f$  is an intrinsic parameter (i.e., independent of concentration), and has been used to characterize the optical properties of DOM in different environments.<sup>28,31–35</sup> For example,  $\Phi_f$  differentiated between effluent organic matter (EffOM) and naturally occurring DOM in wastewater blends with greater statistical power than other optical metrics.<sup>28</sup> Differentiation was ultimately possible because different fluorophores and chromophores existed at different relative abundances in each type of DOM.

While  $\Phi_f$  is a sensitive measure used to quantify the unique fluorescence efficiencies of compounds, only the *apparent*  $\Phi_f$  value of DOM can be determined for bulk-water samples by traditional fluorescence spectroscopy. This is because DOM represents a mixture of absorbing and fluorescing compounds summed by one *apparent*  $\Phi_f$  value, where typical bulk values are in the order of 1-3% and are suppressed by nonfluorescing chromophores.<sup>26,31–33,36</sup> Therefore, to use  $\Phi_f$  to further characterize the DOM mixture it would be useful to fractionate bulk-water DOM from which varying  $\Phi_f$  intensities can be observed for a single sample. It was reported previously that fluorescence to absorbance ratios are MW dependent and that this ratio is greatest for smaller MW fractions.<sup>37–39</sup> Boyle and coworkers also found that, among several DOM samples, the  $\Phi_f$  increased with decreasing sample MW.<sup>40</sup> From these studies it can be seen that: (i)  $\Phi_f$  varies between fractions of a given DOM sample, and (ii)  $\Phi_f$  is likely correlated to DOM MW. It should be noted that throughout the rest of this text, “ $\Phi_f$ ” refers to “*apparent fluorescent quantum yield*”.

This study presents a SEC system in which  $\Phi_f$  is calculated in-line as a function of AMW while in-line total organic carbon (TOC) concentrations measurements are used to identify the presence of spectroscopically undetectable DOM. To do this, dissolved organic carbon concentration (DOC), absorbance, and fluorescence, were combined with a SEC system so that each signal was essentially collected simultaneously as a function of AMW during analysis. To demonstrate the application of the SEC system to characterize the  $\Phi_f$  distribution within DOM, data are presented on the analysis of several DOM samples, consisting of riverine samples and ozonated DOM isolates. The goal of using this system was to better understand the fundamental properties of fluorescence in DOM, while also allowing the investigation of changes to fluorophores across a processing mechanism in natural and engineered systems.

## 2. MATERIALS AND METHODS

## 2.1. Instrumentation

The SEC system was comprised of an Agilent 1260 high performance liquid chromatography (HPLC) setup that included an Agilent 1200 Series Vacuum Degasser, Agilent 1200 Series G1310A Isocratic Pump, Agilent 1260 Infinity Series G1315D Diode Array Detector (DAD), Agilent 1260 Series Infinity II Fluorescence Detectors (FLD) and a Sievers M9 TOC Analyzer. Absorbance and fluorescence signals were recorded directly by the Agilent OpenLab software (Rev. C01.09). An Agilent Universal Interface Box II was utilized to transfer data from the TOC analyzer to the Agilent software in voltage units, which were later converted to DOC concentration ( $\text{mg}_C \text{ L}^{-1}$ ) (see SI, Text S-1.2.3) for a detailed description of conversion). Note that because samples were filtered through  $0.45 \mu\text{m}$  polyethersulfone (PES) filters, analysis results from the TOC analyzer can be considered DOC. A schematic of the instrumental setup for the SEC system is shown in Figure 1.

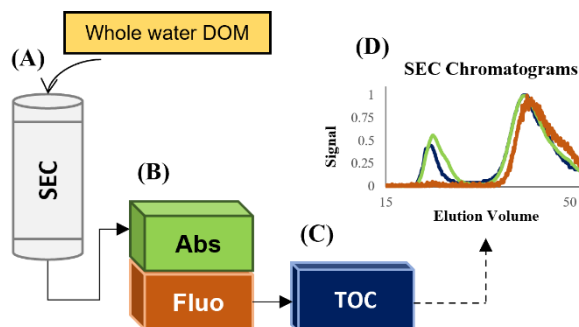


**Figure 1.** Schematic of the size exclusion chromatography (SEC) system. Bulk water samples are injected into the SEC column (A). After eluting from the column, sample passes through the absorbance (Abs) and fluorescence (Fluo) detectors (B) and then travel to the Sievers M9 Total Organic Carbon (TOC) analyzer (C). The in-line coupled system allows for the determination of multiple optical metrics of the dissolved organic matter (DOM) based on apparent molecular weights (AMW), including  $\Phi_f$  (D).

The size-based separations were achieved using a Toyopearl HW-50S column (internal diameter (ID) 20 mm x 25 cm, 92 mL total volume). Samples were injected via an Agilent

Technologies 1100 Series G1328B Manual Injector Assembly with Rheodyne 7725i Injection Valve and 2 mL injection loop. The mobile phase consisted of phosphate buffer (0.0016M Na<sub>2</sub>HPO<sub>4</sub>, 0.0024M NaH<sub>2</sub>PO<sub>4</sub>, and 0.031M Na<sub>2</sub>SO<sub>4</sub>, pH 6.8, ionic strength 0.1M, see SI, Table S1 for a full list of chemicals used and their sources) that was pumped at a flow rate of 1 mL min<sup>-1</sup>. This mobile phase composition aimed to reduce unwanted column interactions and follows the methods of Her and co-workers.<sup>14,41</sup> The Agilent DAD was set to scan from 200-700 nm in 2-nm increments, and the Agilent FLD was operated in multi-emission scan mode at  $\lambda_{\text{ex}} = 350$  nm,  $\lambda_{\text{em}} = 350$ -700 nm at 5-nm increments. These settings were required for accurate spectral corrections (e.g., inner-filter effect corrections) and calculation of  $\Phi_f$  for the different MW fractions of the DOM.

To properly align the different detector signals, salicylic acid (a single compound with well-described absorbance and fluorescence spectra)<sup>21,29,31,32,42</sup> was injected at a concentration of 5 mg L<sup>-1</sup> and peak elution volumes were then used to account for inter-detector volume between absorbance, fluorescence, and DOC detectors. On average, the volumetric difference between the absorbance and fluorescence detectors was approximately 0.05 mL and 2.8 mL between the absorbance and TOC detectors.

All SEC analyses lasted 150 min (total elution volume of 150 mL). Although all of the compounds should theoretically have eluted well before 150 min (void volume and bed volumes for the system were approximately 23 mL and 75 mL), compounds can experience non-ideal interactions causing them to elute after the bed volume.<sup>13,14,43,44</sup> Thus, extra time was utilized to ensure all detectors returned to baseline. Data from the beginning of the run (i.e., before the elution of any compounds) as well as the end of the run (i.e., after the elution of all compounds and all detectors had returned to baseline) were treated as blanks to apply baseline corrections. Following



Her, 2003, the SEC column was initially calibrated with polyethylene glycols (PEG) to ensure results were comparable to previous studies (data not shown).<sup>41</sup> However, discrete molecular weight values or cutoffs were not provided because of the relative nature of SEC. That is, molecular separation is dependent on hydrodynamic size and is affected by solution chemistry and non-ideal interactions within the SEC-column, resulting in differing AMW estimations and AMW distributions.<sup>14,16,43–46</sup> In addition commonly used calibration standards (e.g., polystyrene sulfonates and PEGs)<sup>14,43</sup> are uniform compounds while DOM is a complex mixture of chemically diverse compounds.<sup>45</sup> Therefore, in this study, chromatographic results were presented in terms of elution volume and interpreted qualitatively with respect to AMW (i.e., small, medium, large AMW regions).

Bulk-water characteristics were measured for all samples using a spectrophotometer (Hach DR 6000; Hach, Company, CO, USA), a spectrofluorometer (Horiba Jobin Yvon Fluoromax-4; Horiba, Japan), and a DOC analyzer (Sievers M5310C DOC analyzer; Suez Water Technologies, CO, USA). A full description of the analysis methods is included in the SI, Table S3.

## **2.2 Samples**

A total of nine natural water samples were collected from a subsection of Boulder Creek that flows through the City of Boulder, Colorado, and suburban land surrounding the city, as well as South Boulder Creek near the junction with Boulder Creek (see SI, Figure S1 for exact sample locations). Samples were collected in 250 mL pre-washed and combusted glass bottles, wrapped in foil to exclude light, stored in coolers on ice, and immediately transported to the University of Colorado Boulder. All samples were passed through prewashed 0.45  $\mu\text{m}$  pore size polyethersulfone (PES) filters and transferred into pre-washed and combusted 40 mL amber vials for storage at 4 °C in the dark until analysis. Prior to analysis, 15 mL aliquots of each sample were

spiked with ~1 mL of a concentrated mobile phase solution (0.016M Na<sub>2</sub>HPO<sub>4</sub>, 0.024M NaH<sub>2</sub>PO<sub>4</sub>, and 0.031M Na<sub>2</sub>SO<sub>4</sub>), added dropwise, to match the ionic strength and pH of the mobile phase of the column. In this way, samples are essentially constituted in mobile phase and non-ideal interactions are suppressed as samples exchange into the mobile phase while entering the column after injection.

DOM fulvic acid isolates were obtained from the International Humic Substances Society (IHSS, St. Paul, MN, USA). Suwannee River Fulvic Acid (SRFA, 2S101F) was used as the sample to verify method accuracy and Pony Lake Fulvic Acid (PLFA, 1R109F) was used for ozonation experiments. Stock solutions of ~100 mg<sub>C</sub> L<sup>-1</sup> were prepared in 100 mM phosphate buffer (pH 6.8) for each isolate. The solutions were stirred continuously for 24 hours and then filtered with ultrapure water prewashed 0.45 µm (PES) filters. The exact carbon concentration was measured using a Sievers M5310C DOC analyzer.

For the ozonation experiments, pure oxygen was fed to an ozone (O<sub>3</sub>) generator model TG-40 (Ozone Solutions) and the obtained O<sub>3</sub>/oxygen gas mixture was bubbled into a 2 °C water jacketed 2 L glass reactor filled with ultrapure water. The obtained (O<sub>3</sub>) stock solution had a concentration of ≈ 45 mg<sub>O<sub>3</sub></sub> L<sup>-1</sup> that was measured spectrophotometrically using a 0.2 cm pathlength quartz cell with an absorbance value of 3200 M<sup>-1</sup> cm<sup>-1</sup> at λ=260 nm.<sup>47</sup> Appropriate amounts of the O<sub>3</sub> stock solution were added to 5mg<sub>C</sub> L<sup>-1</sup> PLFA samples to create various specific ozone doses (0.05, 0.1 and 0.2 mmol<sub>O<sub>3</sub></sub> mmol<sub>C</sub><sup>-1</sup>), similar to ozonation steps in drinking or wastewater treatment (0.36–1.16 mg<sub>O<sub>3</sub></sub> mg<sub>C</sub><sup>-1</sup>).

## **2.3 Method Development**

### *2.3.1 Development of Correction Factors for Fluorescence Detector*

Before utilizing the data from the fluorescence detector to calculate  $\Phi_f$ , the spectral bias of monochromators and charge-coupled device detectors had to be considered by applying correction factors. Typically, correction factors are generated by comparing National Institute of Standards and Technology (NIST) certified data of fluorescence standards, such as NIST SRM2942-4 or Rhodamine-B, to the uncorrected fluorescence spectra.<sup>29,48</sup> However, such standards are most commonly solid blocks or come pre-filled into sealed cuvettes, and are incompatible with HPLC detector cells with non-standard dimensions and low volumes. Therefore, this study utilized a method whereby a sample EEM is measured without prior separation (i.e. the analytical column was removed from the system) at a very low flow rate (0.025 mL min<sup>-1</sup>). The low flow rate allows enough time to collect measurements for a single fraction across multiple excitation wavelengths (while entire emission spectra are measured by the Agilent 1260 Infinity Fluorescence Detector). The obtained spectra were then compiled into a SEC-based EEM and compared against the EEM measured on a calibrated stand-alone fluorometer. In our study, the Agilent 1260 Infinity Fluorescence Detector data were compared to the calibrated Horiba Jobin Yvon Fluoromax-4, using SRFA (2S101F) as the standard. SI, Figure S6 shows the obtained correction factors.

### *2.3.2 Verification of In-line Fluorescence Data*

Comparisons of the corrected SRFA EEM measured using the in-line method to the corrected SRFA EEM measured on the reference benchtop fluorometer were made to verify the adequacy of the correction factors (Figure 2). Corrected fluorescence spectra were highly similar at wavelengths with strong emission fluorescence intensities (i.e.  $\lambda_{ex}$ =250-400nm and  $\lambda_{em}$ =350-500nm), while in low emission intensity regions < 350nm, SEC-based EEM signals were relatively noisy. Because the noise occurs in regions where fluorescence signal is typically weak ( $\lambda_{ex}$ >400

nm and  $\lambda_{em} > 550$  nm), and not in the wavelengths used for  $\Phi_f$  calculations, the calculated  $\Phi_f$  are not significantly impacted.

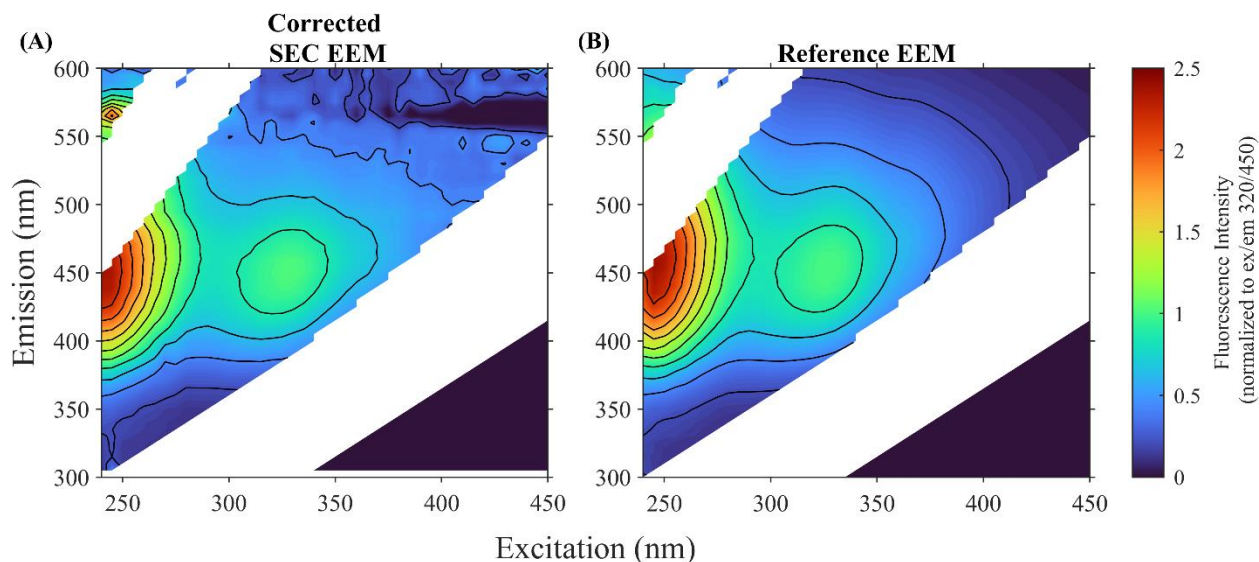


**Figure 2.** Corrected Suwannee River Fulvic Acid (SRFA) sample EEMs from the inline SEC-fluorescence detector (A) and the off-line benchtop fluorometer (B). Excitation wavelengths are plotted on the x-axis and emission wavelengths are plotted on the y-axis. Both EEMs fluorescence intensities (FI) were normalized to excitation 320 and emission 450 nm for a spectral comparison.

Additionally, correction factors were applied to a second reference standard analyzed by the SEC system, quinine sulfate, for which its fluorescence spectrum is well defined. Quinine sulfate has a fluorescence excitation/emission maximum at 347 nm and 455 nm respectively, and well characterized emission in the range of 400-530 nm.<sup>48</sup> The fluorescence spectrum of quinine sulfate overlaps strongly with fluorescence emission of DOM, especially at  $\lambda_{ex}=350$  nm which was the excitation wavelength chosen for this study. For these reasons, quinine sulfate is a good reference standard for DOM research, and commonly used in the field.<sup>21,29</sup> Quinine sulfate was prepared at a concentration of 10 mM in 0.1N H<sub>2</sub>SO<sub>4</sub> and analyzed by the SEC absorbance and fluorescence detectors, using 0.1N H<sub>2</sub>SO<sub>4</sub> as mobile phase. Because the SEC column is limited to a pH range of 2-13, this analysis was conducted with the column removed from the system. Results

are displayed in Figure 3, where the emission spectrum of quinine sulfate is closely replicated, with all data points falling within the error range of the reference spectrum.

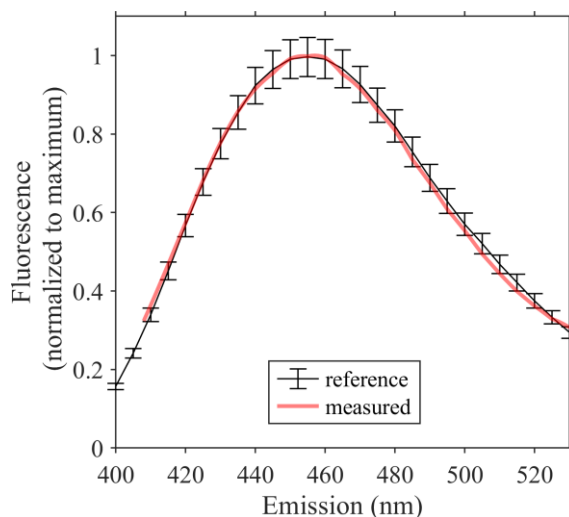


**Figure 3.** Comparison of the corrected SEC quinine sulfate (QS) fluorescence emission spectrum (red) to the referenced spectrum (black). Emission spectra were obtained at  $\lambda_{\text{ex}} = 350$  nm. Fluorescence intensities were normalized to the peak maximum to account for differences in concentration (y-axis).

### 2.3.3 Verification of In-line $\Phi_f$ Calculation

As previously stated,  $\Phi_f$  is defined as the ratio of the number of photons emitted via fluorescence to the number of absorbed photons. The value of  $\Phi_f$  for a compound is calculated by comparison to a standard for which the absolute  $\Phi_f$  is known.<sup>29,30</sup> Standards are typically pure compounds for which the  $\Phi_f$  yield does not vary with excitation wavelength. While quinine sulfate dissolved in  $\text{H}_2\text{SO}_4$  is often used for this purpose,<sup>28,30–32,42</sup> this solution is not compatible with the SEC column (see section 2.3.2). In this study, salicylic acid was used as a  $\Phi_f$  standard as it is well characterized,<sup>31,49</sup> can be readily dissolved in the SEC mobile phase, and thus can be analyzed under the typical instrumental conditions described in Section 2.1. The  $\Phi_f$  values were calculated following eq. 1<sup>42</sup>

$$\frac{\Phi_{f\text{DOM}}}{\Phi_{f\text{SA}}} = \frac{\int_0^\infty I_{\text{DOM}}(\lambda_{\text{ex}}) d\lambda_{\text{em}}}{A_{\text{DOM}}(\lambda_{\text{ex}})} \times \frac{A_{\text{SA}}(\lambda_{\text{ex}})}{\int_0^\infty I_{\text{SA}}(\lambda_{\text{ex}}) d\lambda_{\text{em}}} \quad (1)$$

where  $\Phi_{f,DOM}$  and  $\Phi_{f,SA}$  are the  $\Phi_f$  for DOM and salicylic acid respectively,  $A_{DOM}(\lambda_{ex})$  and  $A_{SA}(\lambda_{ex})$  are the absorbance values of DOM and salicylic acid (at the fluorescence excitation wavelength),  $I_{DOM}(\lambda_{ex})$  and  $I_{SA}(\lambda_{ex})$  indicate the fluorescence intensities at the excitation wavelength and are integrated across the range of emission wavelengths ( $d\lambda_{em}$ ). A 5 mg<sub>C</sub> L<sup>-1</sup> standard of salicylic acid was prepared in mobile phase and analyzed by the SEC system under the same conditions described in section 2.1, and results were compared to the  $\Phi_f$  reference value for salicylic acid.

The measured  $\Phi_f$  for salicylic acid agrees well with a reference value of 36%,<sup>31,49</sup> with deviations less than 4.8% of the reference value (Figure 4). Notably, during data processing,  $\Phi_f$  was calculated only when absorbances were above 0.5 cm<sup>-1</sup>10<sup>-3</sup>; below this threshold, data were noisy and  $\Phi_f$  was unreliable. This was an important limitation for analyzing samples with very low concentrations (i.e., natural water samples, as shown below).

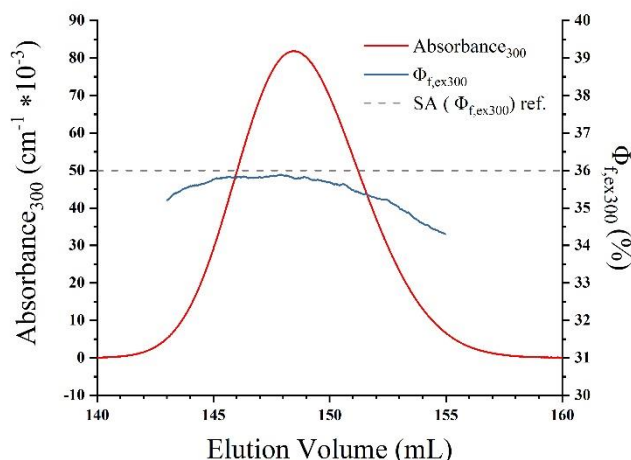


**Figure 4.** Absorbance and fluorescent quantum yield ( $\Phi_f$ ) SEC chromatograms for salicylic acid (SA). Elution volume in mL is plotted on the x-axis, absorbance and percent fluorescent ( $\Phi_f$ ) values are plotted on the primary and secondary y-axes respectively. The red line shows the chromatogram of absorbance at 300 nm, the blue line shows  $\Phi_f$  at  $\lambda_{Ex} = 300$  nm. The reference value for  $\Phi_{f,Ex=300}$  is 36 %, <sup>49</sup> and is shown by the grey dashed line.

### 2.3.3 Verification of Method Accuracy

SRFA was analyzed at two concentrations ( $5.1 \text{ mgC L}^{-1}$  and  $21.5 \text{ mgC L}^{-1}$ ) to verify method accuracy. Specifically it was verified that: (i) SEC chromatographic profiles of the same material are invariant with concentration (i.e., elution volume remains constant), (ii) DOC, absorbance, and fluorescence signals are proportional to concentration for the same sample at different concentrations, <sup>25,50</sup> and (iii)  $\Phi_f$  is independent of concentration <sup>28</sup> (Figure 5). Tucker Congruence Coefficients (TCC) were calculated to compare the normalized chromatograms of the  $5.1 \text{ mgC L}^{-1}$  sample to that of the  $21.5 \text{ mgC L}^{-1}$  for each signal. These TCC values were determined to be 0.998, 0.993, and 0.999 for DOC, absorbance, and fluorescence respectively, indicating excellent agreement ( $\text{TCC} > 0.95$  indicates two components can be considered equal) <sup>51</sup> between normalized chromatograms of the two concentrations (Figure 5.E-G) (refer to SI Text S-2.4 for TCC calculations). The chromatographic peak maximum ratios of DOC, absorbance, and fluorescence (ratios of SRFA chromatographic maximums of two concentrations) for SRFA concentrations are

0.237, 0.242, and 0.257 respectively, representing errors of 3.5, 1.4, and 4.8% (see SI S-2.5 for percent error calculations). The  $\Phi_f$  profiles for the different SRFA concentrations overlay each other indicating that the same  $\Phi_f$  values were calculated for elution volumes ~32-42 mL. However, in Figure 5.D, at ~42 mL,  $\Phi_f$  began to differ between the two concentrations. This results from improved resolution and accuracy of the fluorescence and absorbance signals at higher sample concentration, and not to a change in  $\Phi_f$ , which is an intrinsic property. Thus, for the 5.1 mg<sub>C</sub> L<sup>-1</sup> standard,  $\Phi_f$  signal increased to ~2.5% (at ~45 mL) where it remained (for elution volumes > 45 mL) though signal variance increased. For the 21.5 mg<sub>C</sub> L<sup>-1</sup> standard, two distinct  $\Phi_f$  peaks were seen at ~45 mL and ~52 mL before the signal variance increased.



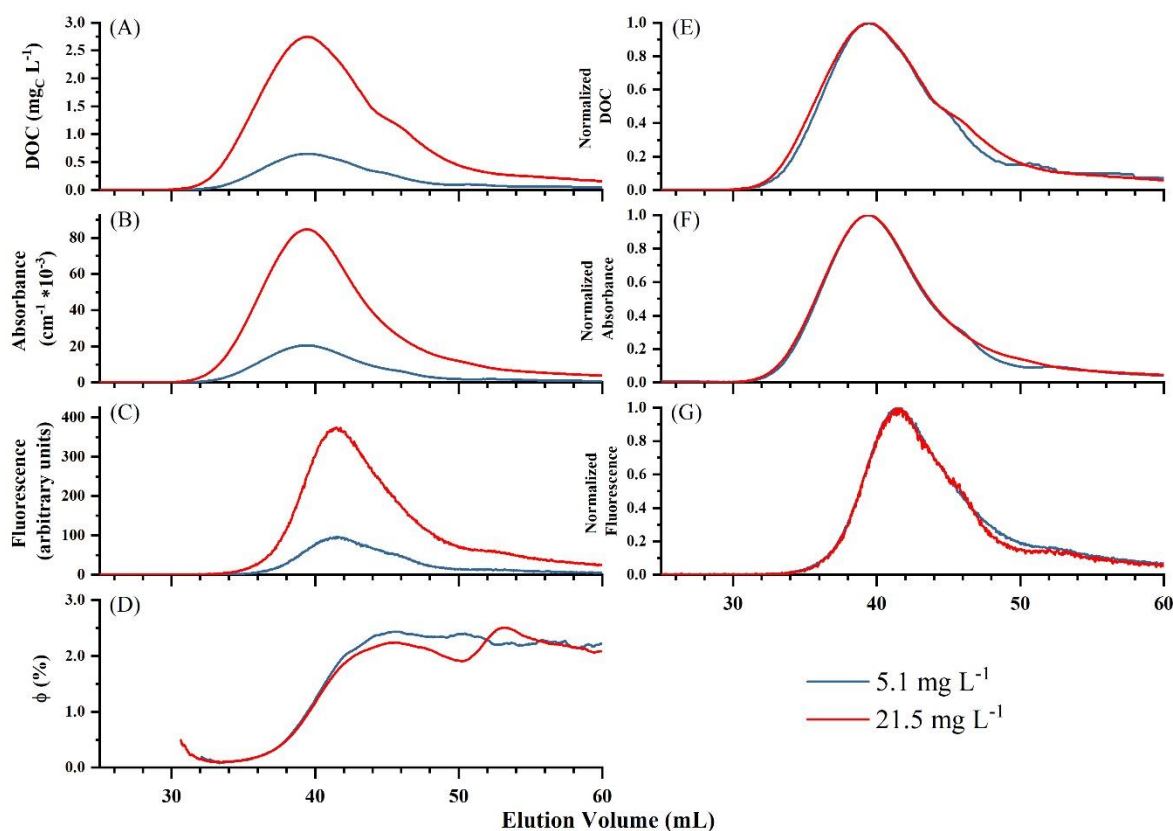


**Figure 5.** SEC chromatograms from the inline system for Suwannee River Fulvic Acid (SRFA: 5.1 and 21.5  $\text{mg}_\text{C} \text{ L}^{-1}$ ). (A) Dissolved organic carbon (DOC), (B) Absorbance ( $\lambda=350 \text{ nm}$ ), (C) Fluorescence ( $\lambda_{\text{ex}}=350 \text{ nm}$ ,  $\lambda_{\text{em}}=390\text{-}700 \text{ nm}$ ), and (D) Fluorescent quantum yield. (E), (F), and (G) show DOC, Absorbance, and Fluorescence chromatograms normalized to the emission peak maximum. Red chromatogram lines show SRFA ( $21.5 \text{ mg}_\text{C} \text{ L}^{-1}$ ) and blue chromatogram lines show SRFA ( $5.1 \text{ mg}_\text{C} \text{ L}^{-1}$ ). Absorbance was obtained at 350 nm, fluorescence and  $\Phi_\text{f}$  were obtained at  $\lambda_{\text{Ex}} = 350 \text{ nm}$ .

### 3. RESULTS AND DISCUSSION

#### 3.1 Applications of coupled SEC system for the Quantification of $\Phi_f$ Distribution

##### 3.1.1 DOM from Boulder Creek

The SEC- $\Phi_f$  method was applied to assess the  $\Phi_f$  distribution for aqueous samples collected from Boulder creek. Figure 6 shows the DOC, absorbance, fluorescence, and  $\Phi_f$  as a function of AMW for a subset of three Boulder Creek samples (SEC data for the additional Boulder Creek and South Boulder Creek samples are provided in SI Figure S7.A-B and bulk water data for all Boulder Creek and South Boulder Creek samples in SI Figures S2-S5, Tables S2-S3). The SEC chromatograms using the DOC detector showed two distinct peaks occurring in elution volume ranges of ~20-30 mL and ~35-50 mL. At sample locations further downstream (streamflow direction is from BC-AF to BC-75<sup>th</sup>), DOC concentration of both peaks (and thus overall DOC concentration) increased (Figure 6). The stream section where BC-AF, BC-61<sup>st</sup>, BC-75<sup>th</sup> samples were taken, flows through an urban corridor of the city of Boulder, therefore, it is likely that a complex combination of anthropogenic inputs are responsible for the observed increases in DOC concentrations downstream.<sup>52,53</sup>

Absorbance chromatograms also displayed two distinct peaks within 20-30 mL and 35-50 mL, while fluorescence chromatograms show one peak within 35-50 mL. For the remainder of the discussion, the absorbance peaks within 20-30 mL and 35-50 mL will be referred to as “large AMW” and “medium to small AMW” peaks, respectively. Thus, chromophoric compounds (absorbing at 350 nm) contributed to both peaks, while fluorophores (excited at 350 nm) were constrained to the medium to small AMW peak. It has been reported elsewhere that, upon fractionation by AMW, a distinction is observed between large AMW fractions with high absorbance (i.e., the fluorescence:absorbance ratio is small), and small AMW fractions with

intense fluorescence (i.e., the fluorescence:absorbance ratio is large).<sup>37,38</sup> Interestingly, in the medium to small AMW peak, where absorbance and fluorescence signals are greatest, the absorbance and fluorescence peaks vary much less between samples than the DOC, indicating the differences between DOC chromatograms were largely due to nonchromophoric DOM (i.e., spectroscopically invisible).

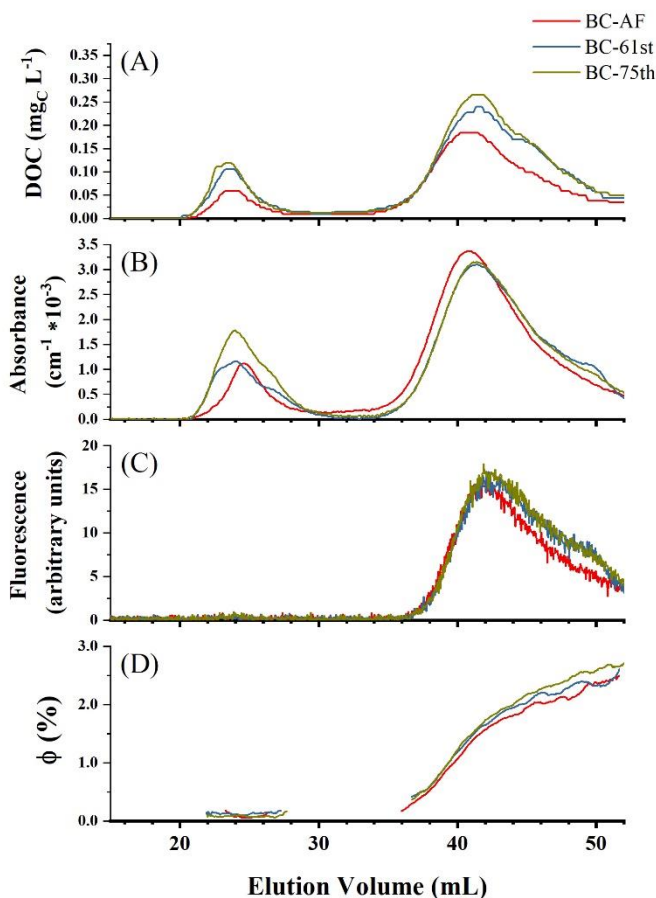


**Figure 6:** SEC chromatograms for Boulder Creek water samples. (A) Dissolved Organic Carbon (DOC), (B) Absorbance ( $\lambda=350$  nm), (C) Fluorescence ( $\lambda_{\text{ex}}=350$  nm,  $\lambda_{\text{em}}=390-700$  nm), and (D) Fluorescent quantum yield ( $\Phi_f$ ).  $\Phi_f$  was not calculated when absorbance was below  $0.5 \text{ cm}^{-1} 10^{-3}$ . Red lines show the sample from Boulder Creek at 61<sup>st</sup> Street (BC-61<sup>st</sup>), blue lines show the sample from Boulder Creek at Arapahoe Avenue (BC-AF), and yellow lines show the sample from Boulder Creek at 75<sup>th</sup> Street (BC-75<sup>th</sup>). Absorbance was measured at 350 nm, fluorescence and  $\Phi_f$  were measured at  $\lambda_{\text{Ex}} = 350$  nm.

The  $\Phi_f$  results for Boulder Creek samples are shown in Figure 6.D. The  $\Phi_f$  was calculated in the elution volume range in which absorbance intensities were above  $0.5 \text{ cm}^{-1} \times 10$ . Across elution volumes  $\sim 35$ - $53$  mL,  $\Phi_f$  increased from  $<0.5\%$  to  $\sim 2.5\%$  for smaller AMW fractions (earlier elution volumes) relative to larger AMW fractions (later elution volumes), where bulk water  $\Phi_f$  values for the same samples were determined to be  $0.97$ - $1.39\%$  (SI, Figure S5). These data indicate that although most absorbance and fluorescence (as a fraction of the overall DOM absorbance and fluorescence) occurred between  $38$ - $46$  mL (where signal intensities increased to a chromatographic maximum at  $\sim 40$ - $42$  mL before decreasing with increasing elution volumes), the  $\Phi_f$  values continued to increase with increasing elution volumes of medium to small AMW fractions.

Prior research has been dedicated to understanding the structural properties of chromophores and fluorophores within DOM.<sup>18,50,54,55</sup> Although some correlations on the structural identities of these optically active species (phenols, quinones, etc.) have been made,<sup>22,56-59</sup> their distribution within the DOM molecular size continuum is not well understood.<sup>31,60</sup> The data presented here provides the first direct evidence of a clear separation between weakly fluorescing species present at higher concentrations (thus observed with relatively higher fluorescence and lower  $\Phi_f$  signal intensities) eluting between  $38$ - $46$  mL, as opposed to highly fluorescing species which dominate the lower AMW fractions, though their overall mass contributions are smaller (observed with lower fluorescence and higher  $\Phi_f$  signal intensities). This de-coupling between numerous weakly fluorescent fractions with relatively larger AMW, and fewer highly fluorescent fractions with relatively lower AMW, matches well with other work where the  $\Phi_f$  MW distribution was assessed.<sup>37,38,40</sup> It should be noted that this study analyzed the AMW distribution of  $\Phi_f$  only at  $\lambda_{\text{Ex}} = 350$  nm. Future studies may benefit from exploring the relationship at other relevant  $\lambda_{\text{Ex}}$ .

Figure 7 displays SEC-based DOC, absorbance, fluorescence, and  $\Phi_f$  chromatograms for one Boulder Creek sample (BC 75<sup>th</sup>) to help understand the qualitative DOM behavior observed for  $\Phi_f$ . While the absorbance trace closely mirrored the DOC in both shape and elution volume, fluorescence material with smaller AMWs eluted with a similar, but slightly offset size distribution. This suggests that within the medium to small AMW range, as the AMW decreased, DOM fluorescence increased relative to absorbance at  $\lambda_{ex}=350$  nm. This observation highlights the ability of SEC measurements to provide a more in-depth understanding of the complex composition of DOM, with respect to  $\Phi_f$ .

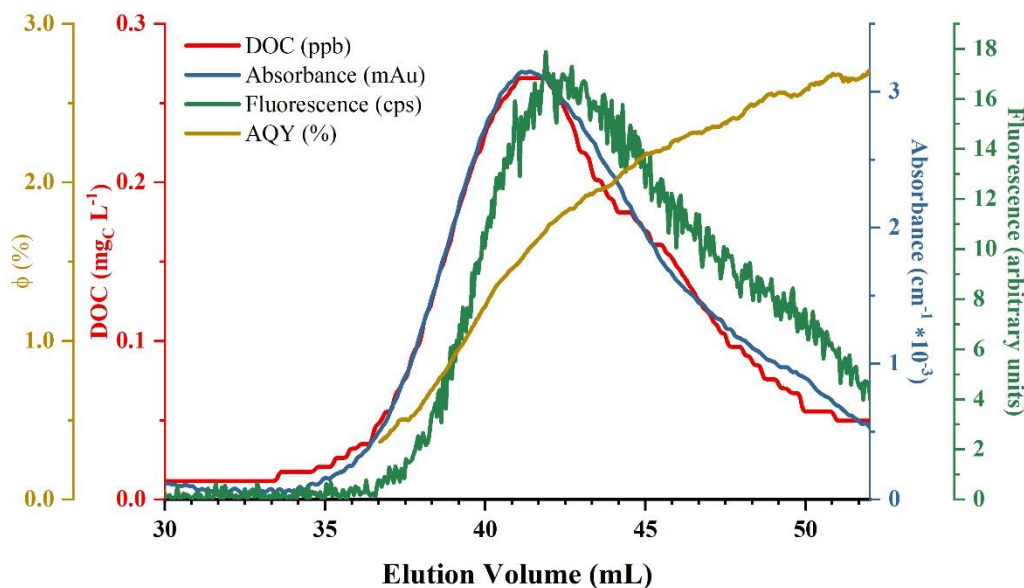


**Figure 7:** SEC chromatograms for Boulder Creek sample BC-75<sup>th</sup> in the medium to low apparent molecular weight (AMW) range. Dissolved Organic Carbon (DOC), absorbance ( $\lambda=350$  nm), fluorescence ( $\lambda_{ex}=350$  nm,  $\lambda_{em}=390-700$  nm), and  $\Phi_f$  are plotted on the red, blue, green, and yellow y-axes, respectively. Absorbance was measured at 350 nm, fluorescence and  $\Phi_f$  were measured at  $\lambda_{Ex} = 350$  nm.

### 3.1.2. Impact of Ozonation on PLFA

Section 3.1.1 presented an application of this method along a biogeochemical gradient. In this section, we describe the impact of a chemical process (ozonation) on DOM properties and  $\Phi_f$ . Solutions of PLFA ( $5 \text{ mg}_C \text{ L}^{-1}$ ) were ozonated at ozone doses of 0.05, 0.1, and  $0.2 \text{ mmol}_{O_3} \text{ mmol}_C^{-1}$ . Previous research indicates that ozonation of PLFA induces a decrease in absorbance and fluorescence, but an increase in  $\Phi_f$ .<sup>61,62</sup> Upon ozonation, bulk water DOC changes only minimally,<sup>63</sup> but low AMW products are formed such as formaldehyde, acetaldehyde, or oxalic acid,<sup>64</sup> that should be observable by the SEC-DOC detector. The fact that DOC, absorbance, fluorescence, and  $\Phi_f$  all change as a result of ozonation, suggests that SEC coupled with DOC, absorbance, and fluorescence detection would prove a valuable tool to follow the changes induced by ozonation.

With increasing ozone doses, a decrease in absorbance and fluorescence in PLFA was observed (Figure 8.B-C). The DOC chromatograms indicate that there was a reduction in large AMW compounds ( $< \sim 40 \text{ mL}$ ), and a simultaneous increase in smaller AMW compounds ( $\sim 40$ - $53 \text{ mL}$ ) with formation of two distinct lower AMW peaks at  $\sim 45$  and  $\sim 52 \text{ mL}$  (Figure 8.A,E). Additionally, the normalized (to the maximum) absorbance and fluorescence chromatograms are presented in Figure 8.E-F. Interestingly, while both absorbance and fluorescence values across the associated chromatograms decreased, the normalized data revealed that with increasing ozone dose, the absorbance trace shifted to lower AMW, while the fluorescence trace remained roughly distributed over the same AMW range. As a result, the SEC- $\Phi_f$  showed a larger increase for large AMW molecules ( $\sim 33$ - $40 \text{ mL}$ ) while the increase was less significant for smaller AMW ( $> \sim 40 \text{ mL}$ ) (Figure 8.D). Previous research observed increasing bulk  $\Phi_f$  with increasing ozone doses.<sup>61</sup> This observation is confirmed here in more detail, in which the increase is particularly marked for the high AMW fraction ( $< \sim 40 \text{ mL}$ ).

Ozonation of phenols leads to the formation of ring-opening products, indicating that carbon-carbon bonds can be broken by ozonation.<sup>65</sup> The DOC chromatograms indicate that ozonation induces a fragmentation of DOM molecules, an observation that concords with the breaking of carbon-carbon bonds and the aforementioned appearance of low AMW products such as formaldehyde, acetaldehyde, and oxalic acid.<sup>64</sup> The remaining fluorescence after ozone treatment is indicative of functional groups that are not as reactive with ozone, and could include terpenoids or phenols with a high  $pK_a$  (the deprotonated form of phenol being more reactive by  $\approx$  4-6 orders of magnitude towards ozone). An example of such a phenol is salicylic acid, which has a  $pK_a$  for the phenolic moieties of 13.4.<sup>47</sup>

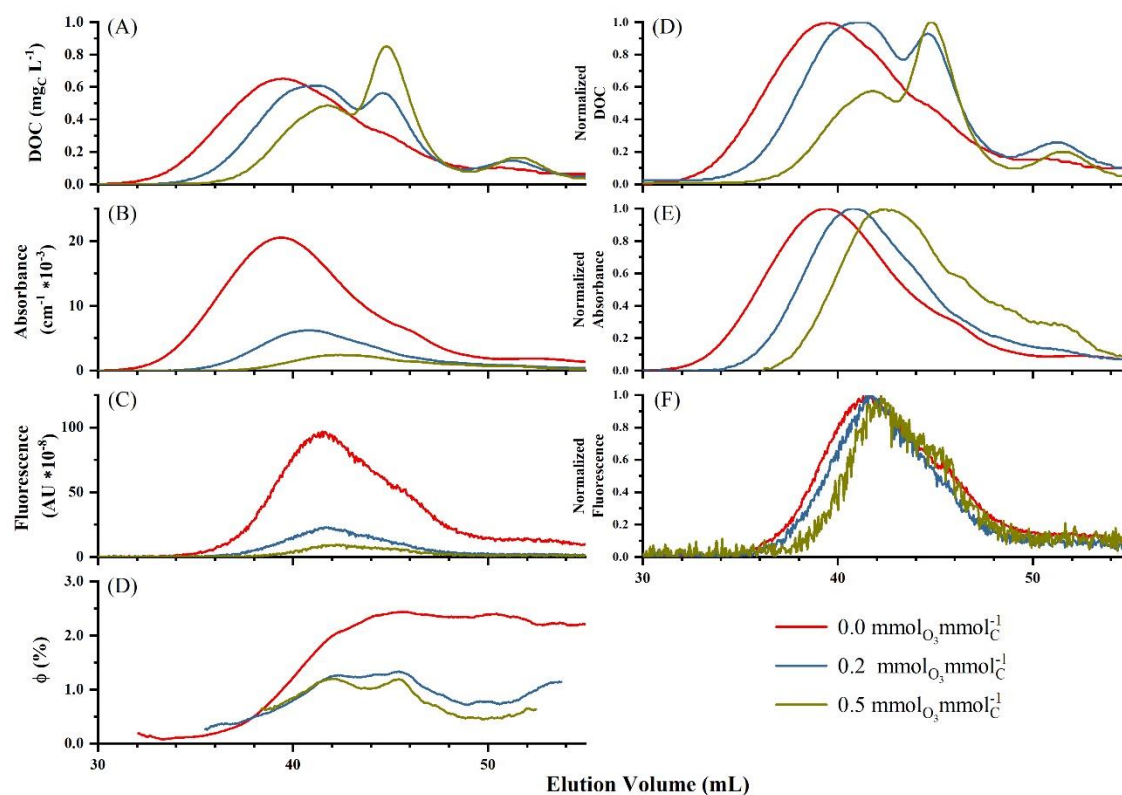


**Figure 8:** Left: Dissolved Organic Carbon (DOC), absorbance ( $\lambda=350$  nm), fluorescence ( $\lambda_{ex}=350$  nm,  $\lambda_{em}=390-700$  nm), and  $\Phi_f$  chromatograms for PLFA ( $5 \text{ mgC L}^{-1}$ ) samples treated with ozone. (A) DOC ( $\text{mgC L}^{-1}$ ), (B) Absorbance, (C) Fluorescence, and (D) Fluorescent quantum yield chromatograms. Right: Normalized absorbance and fluorescence chromatograms for PLFA treated with ozone. (D) DOC chromatograms normalized to the peak maximum. (E) Absorbance

chromatograms normalized to the chromatogram peak maximum (i.e., normalized to 1). (F) Fluorescence chromatograms normalized to the chromatogram peak maximum. **All plots:** The red line shows untreated PLFA, the yellow line shows PLFA ozonated at a dose of 0.05 mmol<sub>O<sub>3</sub></sub> mmol<sub>C</sub><sup>-1</sup>, the blue line shows PLFA ozonated at a dose of 0.1 mmol<sub>O<sub>3</sub></sub> mmol<sub>C</sub><sup>-1</sup>, and the green line shows PLFA ozonated at a dose of 0.2 mmol<sub>O<sub>3</sub></sub> mmol<sub>C</sub><sup>-1</sup>. Chromatograms were plotted as a function of elution volume (mL).

### 3.2 Further Potential Applications

Although the focus of this work was on calculating the  $\Phi_f$  for AMW fractions from SEC analysis, the system as developed, could be used to calculate a variety of additional optical parameters. Examples that have previously been used in the investigation of bulk water DOM include: SUVA<sub>254</sub>, spectral slopes, specific fluorescence, fluorescence indices, and fluorescence peak ratios.<sup>54,66–71</sup> Coupling these metrics with SEC analysis would lead to a more complete understanding of physiochemical properties of DOM as a function of MW. Additionally, recent work by Ulliman et al. (2020) proposed a methodology to evaluate the potential for several parameters (e.g.,  $\Phi_f$ , fluorescence peak ratios A:C and C:T, fluorescence peak T intensity, and fluorescence index) to differentiate natural DOM from EffOM using several paired samples.<sup>28</sup> A similar methodology can be applied to the same parameters coupled with SEC. Because SEC fractionates samples by size, it reduces the complexity of DOM with respect to bulk water analysis. We suggest that future work using this system could investigate whether this reduced complexity extends to other freshwater, marine, and soil porewaters, leading to a greater ability to differentiate DOM qualitative changes and DOM sources. Furthermore, this method provides a means by which highly fluorescent size fractions of DOM can be identified for more detailed analyses of carbon quality and its changes through different processing mechanisms. This system was specifically developed to capture different fractions for further off-line biological and chemical analysis at the



molecular level using other analytical techniques (e.g., high resolution mass spectrometry and nuclear magnetic resonance spectroscopy).

#### 4. CONCLUSION

This study developed a novel in-line method for the determination of  $\Phi_f$  as a function of AMW using a SEC system coupled with DOC, absorbance, and fluorescence. This method provides useful and important information regarding DOM characterization, especially regarding fluorescence properties, something that still is considered to be a black-box in the DOM characterization community. The development and validation of instrument-specific correction factors for the SEC-fluorescence detector were needed to produce accurate fluorescence emission spectra. We calculated the  $\Phi_f$  with the help of a salicylic acid standard, confirmed method accuracy by varying concentrations, and monitored chemical processing effects of ozonation for different AMW DOM fractions.  $\Phi_f$  of the DOM in natural water and fulvic isolate samples followed a characteristic profile whereby  $\Phi_f$  increased with decreasing AMW. However, the profile of PLFA DOM changed following ozonation, suggesting SEC-based  $\Phi_f$  tracks important fundamental changes to DOM composition.

For all sample sets, a close investigation of all chromatographic results (fluorescence, absorbance, and DOC) individually, is especially useful in the qualitative understanding of sample composition and chromatographic behavior. For example, the natural water samples and the isolates analyzed in this study showed that larger AMW fractions with lower  $\Phi_f$  correspond with higher DOC concentrations while smaller AMW fractions with higher  $\Phi_f$  correspond with lower concentrations. While DOM components with higher  $\Phi_f$  will contribute more to observed bulk fluorescence than components with lower  $\Phi_f$  relative to their abundances, bulk water  $\Phi_f$  values are weighted more heavily to lower SEC-based  $\Phi_f$  (<1.5%) due to higher abundances (i.e.,

concentration). Additionally, by comparing the SEC-DOC to SEC-absorbance and SEC-DOC to SEC-fluorescence signals, it can be understood which fractions contain DOM that is chromophoric and fluorophoric and which fractions are not, providing more detail than is detected by bulk water absorbance and fluorescence analysis alone. Finally, it is proposed that future studies could utilize this method to differentiate between sources of OM (e.g., natural organic matter from diverse ecosystems and EffOM), and to identify highly fluorescent components for isolation and further detailed investigation.

## **5. ACKNOWLEDGEMENTS**

Funding for this project came from Suez Water Technologies, Boulder, CO. We thank Brett Clark and Amanda Scott for additional advisement over the development of size exclusion chromatography methodology. We would like to thank Philip Wenig for providing the essential software tool to export fluorescence scans from the proprietary instrument software format. Funding was also provided by the US National Science Foundation (Awards 1804704, 1804736, and 2027431). KRM acknowledges funding from Svenska Forskningsrådet Formas, Grant 2017-00743.

## **Supporting Information**

Additional materials and methods including a table of chemicals used, sample collection information, and a map of sample locations, additional results and discussion including bulk water analysis results, additional sample results not presented in the main text, details of statistical analysis, and a weighted integration of online SEC-based fluorescent quantum yield from the ozone experiment.

## 6. REFERENCES

- (1) Bauer, J. E.; Cai, W.-J.; Raymond, P. A.; Bianchi, T. S.; Hopkinson, C. S.; Regnier, P. A. G. The Changing Carbon Cycle of the Coastal Ocean. *Nature* **2013**, *504* (7478), 61–70. <https://doi.org/10.1038/nature12857>.
- (2) Bianchi, T. S. The Role of Terrestrially Derived Organic Carbon in the Coastal Ocean: A Changing Paradigm and the Priming Effect. *Proceedings of the National Academy of Sciences* **2011**, *108* (49), 19473–19481. <https://doi.org/10.1073/pnas.1017982108>.
- (3) Azam, F.; Fenchel, T.; Field, J. G.; Gray, J. S.; Meyer-Reil, L. A.; Thingstad, F. The Ecological Role of Water-Column Microbes in the Sea. *Marine Ecology Progress Series* **1983**, *10*, 257–263. <https://doi.org/10.3354/meps010257>.
- (4) Ravichandran, M. Interactions between Mercury and Dissolved Organic Matter—a Review. *Chemosphere* **2004**, *55* (3), 319–331. <https://doi.org/10.1016/j.chemosphere.2003.11.011>.
- (5) Nikolaou, A. D.; Lekkas, T. D. The Role of Natural Organic Matter during Formation of Chlorination By-Products: A Review. *Acta hydrochimica et hydrobiologica* **2001**, *29* (2–3), 63–77. [https://doi.org/10.1002/1521-401X\(200109\)29:2/3<63::AID-AHEH63>3.0.CO;2-C](https://doi.org/10.1002/1521-401X(200109)29:2/3<63::AID-AHEH63>3.0.CO;2-C).
- (6) Singer, P. C. Humic Substances as Precursors for Potentially Harmful Disinfection By-Products. *Water Science and Technology* **1999**, *40* (9), 25–30. [https://doi.org/10.1016/S0273-1223\(99\)00636-8](https://doi.org/10.1016/S0273-1223(99)00636-8).
- (7) Perdue, E. M.; Ritchie, J. D. 5.10 - Dissolved Organic Matter in Freshwaters. In *Treatise on Geochemistry*; Holland, H. D., Turekian, K. K., Eds.; Pergamon: Oxford, 2003; pp 273–318. <https://doi.org/10.1016/B0-08-043751-6/05080-5>.
- (8) Aiken, G. R.; Malcolm, R. L. Molecular Weight of Aquatic Fulvic Acids by Vapor Pressure Osmometry. *Geochimica et Cosmochimica Acta*, 1987, *51*, 8.
- (9) Pavlik, J. W.; Perdue, E. M. Number-Average Molecular Weights of Natural Organic Matter, Hydrophobic Acids, and Transphilic Acids from the Suwannee River, Georgia, as Determined Using Vapor Pressure Osmometry. *Environmental Engineering Science* **2015**, *32* (1), 23–30. <https://doi.org/10.1089/ees.2014.0269>.
- (10) Appiani, E.; Page, S. E.; McNeill, K. On the Use of Hydroxyl Radical Kinetics to Assess the Number-Average Molecular Weight of Dissolved Organic Matter. *Environ. Sci. Technol.* **2014**, *48* (20), 11794–11802. <https://doi.org/10.1021/es5021873>.
- (11) McAdams, B. C.; Aiken, G. R.; McKnight, D. M.; Arnold, W. A.; Chin, Y.-P. High Pressure Size Exclusion Chromatography (HPSEC) Determination of Dissolved Organic Matter Molecular Weight Revisited: Accounting for Changes in Stationary Phases, Analytical Standards, and Isolation Methods. *Environ. Sci. Technol.* **2018**, *52* (2), 722–730. <https://doi.org/10.1021/acs.est.7b04401>.
- (12) Remucal, C. K.; Cory, R. M.; Sander, M.; McNeill, K. Low Molecular Weight Components in an Aquatic Humic Substance As Characterized by Membrane Dialysis and Orbitrap Mass Spectrometry. *Environ. Sci. Technol.* **2012**, *46* (17), 9350–9359. <https://doi.org/10.1021/es302468q>.
- (13) Huber, S. A.; Balz, A.; Abert, M.; Pronk, W. Characterisation of Aquatic Humic and Non-Humic Matter with Size-Exclusion Chromatography – Organic Carbon Detection – Organic Nitrogen Detection (LC-OCD-OND). *Water Research* **2011**, *45* (2), 879–885. <https://doi.org/10.1016/j.watres.2010.09.023>.
- (14) Her, N.; Amy, G.; Foss, D.; Cho, J.; Yoon, Y.; Kosenka, P. Optimization of Method for Detecting and Characterizing NOM by HPLC–Size Exclusion Chromatography with UV and On-Line DOC Detection. *Environ. Sci. Technol.* **2002**, *36* (5), 1069–1076. <https://doi.org/10.1021/es015505j>.
- (15) Cabaniss, S. E.; Zhou, Q.; Maurice, P. A.; Chin, Y.-P.; Aiken, G. R. A Log-Normal Distribution Model for the Molecular Weight of Aquatic Fulvic Acids. *Environ. Sci. Technol.* **2000**, *34* (6), 1103–1109. <https://doi.org/10.1021/es990555y>.
- (16) Hawkes, J. A.; Sjöberg, P. J. R.; Bergquist, J.; Tranvik, L. J. Complexity of Dissolved Organic Matter in the Molecular Size Dimension: Insights from Coupled Size Exclusion Chromatography

- Electrospray Ionisation Mass Spectrometry. *Faraday Discuss.* **2019**, 218 (0), 52–71.  
<https://doi.org/10.1039/C8FD00222C>.
- (17) Coble, P. G.; Green, S. A.; Blough, N. V.; Gagosian, R. B. Characterization of Dissolved Organic Matter in the Black Sea by Fluorescence Spectroscopy. *Nature* **1990**, 348 (6300), 432–435.  
<https://doi.org/10.1038/348432a0>.
  - (18) Coble, P. G. Characterization of Marine and Terrestrial DOM in Seawater Using Excitation-Emission Matrix Spectroscopy. *Marine Chemistry* **1996**, 51 (4), 325–346.  
[https://doi.org/10.1016/0304-4203\(95\)00062-3](https://doi.org/10.1016/0304-4203(95)00062-3).
  - (19) Henderson, R. K.; Baker, A.; Murphy, K. R.; Hambly, A.; Stuetz, R. M.; Khan, S. J. Fluorescence as a Potential Monitoring Tool for Recycled Water Systems: A Review. *Water Research* **2009**, 43 (4), 863–881. <https://doi.org/10.1016/j.watres.2008.11.027>.
  - (20) Murphy, K. R.; Stedmon, C. A.; Waite, T. D.; Ruiz, G. M. Distinguishing between Terrestrial and Autochthonous Organic Matter Sources in Marine Environments Using Fluorescence Spectroscopy. *Marine Chemistry* **2008**, 108 (1), 40–58. <https://doi.org/10.1016/j.marchem.2007.10.003>.
  - (21) Korak, J. A.; Dotson, A. D.; Summers, R. S.; Rosario-Ortiz, F. L. Critical Analysis of Commonly Used Fluorescence Metrics to Characterize Dissolved Organic Matter. *Water Research* **2014**, 49, 327–338. <https://doi.org/10.1016/j.watres.2013.11.025>.
  - (22) D’Andrilli, J.; Foreman, C. M.; Marshall, A. G.; McKnight, D. M. Characterization of IHSS Pony Lake Fulvic Acid Dissolved Organic Matter by Electrospray Ionization Fourier Transform Ion Cyclotron Resonance Mass Spectrometry and Fluorescence Spectroscopy. *Organic Geochemistry* **2013**, 65, 19–28. <https://doi.org/10.1016/j.orggeochem.2013.09.013>.
  - (23) Fischer, S. J.; Gonsior, M.; Chorover, J.; Powers, L. C.; Hamilton, A.; Ramirez, M.; Torrents, A. Biosolids Leachate Variability, Stabilization Surrogates, and Optical Metric Selection. *Environ. Sci.: Water Res. Technol.* **2022**, 8 (3), 657–670. <https://doi.org/10.1039/D1EW00320H>.
  - (24) Leenheer, J. A. Systematic Approaches to Comprehensive Analyses of Natural Organic Matter. *Annals of Environmental Science* **2009**, 3.
  - (25) *Aquatic Organic Matter Fluorescence*; Coble, P. G., Lead, J., Baker, A., Reynolds, D. M., Spencer, R. G. M., Eds.; Cambridge Environmental Chemistry Series; Cambridge University Press: Cambridge, 2014. <https://doi.org/10.1017/CBO9781139045452>.
  - (26) Korak, J. A.; Rosario-Ortiz, F. L.; Summers, R. S. Evaluation of Optical Surrogates for the Characterization of DOM Removal by Coagulation. *Environ. Sci.: Water Res. Technol.* **2015**, 1 (4), 493–506. <https://doi.org/10.1039/C5EW00024F>.
  - (27) Stedmon, C. A.; Nelson, N. B. Chapter 10 - The Optical Properties of DOM in the Ocean. In *Biogeochemistry of Marine Dissolved Organic Matter (Second Edition)*; Hansell, D. A., Carlson, C. A., Eds.; Academic Press: Boston, 2015; pp 481–508. <https://doi.org/10.1016/B978-0-12-405940-5.00010-8>.
  - (28) Ulliman, S. L.; Korak, J. A.; Linden, K. G.; Rosario-Ortiz, F. L. Methodology for Selection of Optical Parameters as Wastewater Effluent Organic Matter Surrogates. *Water Research* **2020**, 170, 115321. <https://doi.org/10.1016/j.watres.2019.115321>.
  - (29) Lakowics, J. R. *Principles of Fluorescence Spectroscopy*; 2006.
  - (30) Würth, C.; Grabolle, M.; Pauli, J.; Spieles, M.; Resch-Genger, U. Comparison of Methods and Achievable Uncertainties for the Relative and Absolute Measurement of Photoluminescence Quantum Yields. *Anal. Chem.* **2011**, 83 (9), 3431–3439. <https://doi.org/10.1021/ac2000303>.
  - (31) Wünsch, U. J.; Murphy, K. R.; Stedmon, C. A. Fluorescence Quantum Yields of Natural Organic Matter and Organic Compounds: Implications for the Fluorescence-Based Interpretation of Organic Matter Composition. *Frontiers in Marine Science* **2015**, 2.
  - (32) Del Vecchio, R.; Blough, N. V. On the Origin of the Optical Properties of Humic Substances. *Environ. Sci. Technol.* **2004**, 38 (14), 3885–3891. <https://doi.org/10.1021/es049912h>.
  - (33) McKay, G.; Korak, J. A.; Erickson, P. R.; Latch, D. E.; McNeill, K.; Rosario-Ortiz, F. L. The Case Against Charge Transfer Interactions in Dissolved Organic Matter Photophysics. *Environ. Sci. Technol.* **2018**, 52 (2), 406–414. <https://doi.org/10.1021/acs.est.7b03589>.

- (34) Mostafa, S.; Korak, J. A.; Shimabuku, K.; Glover, C. M.; Rosario-Ortiz, F. L. Relation between Optical Properties and Formation of Reactive Intermediates from Different Size Fractions of Organic Matter. In *Advances in the Physicochemical Characterization of Dissolved Organic Matter: Impact on Natural and Engineered Systems*; ACS Symposium Series; American Chemical Society, 2014; Vol. 1160, pp 159–179. <https://doi.org/10.1021/bk-2014-1160.ch008>.
- (35) Green, S. A.; Blough, N. V. Optical Absorption and Fluorescence Properties of Chromophoric Dissolved Organic Matter in Natural Waters. *Limnology and Oceanography* **1994**, *39* (8), 1903–1916. <https://doi.org/10.4319/lo.1994.39.8.1903>.
- (36) Brucoleri, A.; Pant, B. C.; Sharma, D. K.; Langford, C. H. Evaluation of Primary Photoproduct Quantum Yields in Fulvic Acid. *Environ. Sci. Technol.* **1993**, *27* (5), 889–894. <https://doi.org/10.1021/es00042a011>.
- (37) Stewart, A. J.; Wetzel, R. G. Fluorescence: Absorbance Ratios—a Molecular-Weight Tracer of Dissolved Organic Matter1. *Limnology and Oceanography* **1980**, *25* (3), 559–564. <https://doi.org/10.4319/lo.1980.25.3.0559>.
- (38) De Haan, H.; De Boer, T. Applicability of Light Absorbance and Fluorescence as Measures of Concentration and Molecular Size of Dissolved Organic Carbon in Humic Lake Tjeukemeer. *Water Research* **1987**, *21* (6), 731–734. [https://doi.org/10.1016/0043-1354\(87\)90086-8](https://doi.org/10.1016/0043-1354(87)90086-8).
- (39) Wünsch, U. J.; Stedmon, C. A.; Tranvik, L. J.; Guillemette, F. Unraveling the Size-Dependent Optical Properties of Dissolved Organic Matter. *Limnology and Oceanography* **2018**, *63* (2), 588–601. <https://doi.org/10.1002/lno.10651>.
- (40) Boyle, E. S.; Guerriero, N.; Thiallet, A.; Vecchio, R. D.; Blough, N. V. Optical Properties of Humic Substances and CDOM: Relation to Structure. *Environ. Sci. Technol.* **2009**, *43* (7), 2262–2268. <https://doi.org/10.1021/es803264g>.
- (41) Her, N.; Amy, G.; McKnight, D.; Sohn, J.; Yoon, Y. Characterization of DOM as a Function of MW by Fluorescence EEM and HPLC-SEC Using UVA, DOC, and Fluorescence Detection. *Water Research* **2003**, *37* (17), 4295–4303. [https://doi.org/10.1016/S0043-1354\(03\)00317-8](https://doi.org/10.1016/S0043-1354(03)00317-8).
- (42) Cawley, K. M.; Korak, J. A.; Rosario-Ortiz, F. L. Quantum Yields for the Formation of Reactive Intermediates from Dissolved Organic Matter Samples from the Suwannee River. *Environmental Engineering Science* **2015**, *32* (1), 31–37. <https://doi.org/10.1089/ees.2014.0280>.
- (43) Sandron, S.; Rojas, A.; Wilson, R.; Davies, N. W.; Haddad, P. R.; Shellie, R. A.; Nesterenko, P. N.; Kelleher, B. P.; Paull, B. Chromatographic Methods for the Isolation, Separation and Characterisation of Dissolved Organic Matter. *Environ. Sci.: Processes Impacts* **2015**, *17* (9), 1531–1567. <https://doi.org/10.1039/C5EM00223K>.
- (44) Hutta, M.; Góra, R.; Halko, R.; Chalányová, M. Some Theoretical and Practical Aspects in the Separation of Humic Substances by Combined Liquid Chromatography Methods. *Journal of Chromatography A* **2011**, *1218* (49), 8946–8957. <https://doi.org/10.1016/j.chroma.2011.06.107>.
- (45) Wünsch, U. J.; Murphy, K. R.; Stedmon, C. A. The One-Sample PARAFAC Approach Reveals Molecular Size Distributions of Fluorescent Components in Dissolved Organic Matter. *Environ. Sci. Technol.* **2017**, *51* (20), 11900–11908. <https://doi.org/10.1021/acs.est.7b03260>.
- (46) Conte, P.; Piccolo, A. High Pressure Size Exclusion Chromatography (HPSEC) of Humic Substances: Molecular Sizes, Analytical Parameters, and Column Performance. *Chemosphere* **1999**, *38* (3), 517–528. [https://doi.org/10.1016/S0045-6535\(98\)00198-2](https://doi.org/10.1016/S0045-6535(98)00198-2).
- (47) von Sonntag, C.; von Gunten, U. *Chemistry of Ozone in Water and Wastewater Treatment: From Basic Principles to Applications*; 2012. <https://doi.org/10.2166/9781780400839>.
- (48) Velapoldi, R. A.; Tønnesen, H. H. Corrected Emission Spectra and Quantum Yields for a Series of Fluorescent Compounds in the Visible Spectral Region. *Journal of Fluorescence* **2004**, *14* (4), 465–472. <https://doi.org/10.1023/B:JOFL.0000031828.96368.c1>.
- (49) Pozdnyakov, I. P.; Pigliucci, A.; Tkachenko, N.; Plyusnin, V. F.; Vauthey, E.; Lemmetyinen, H. The Photophysics of Salicylic Acid Derivatives in Aqueous Solution. *Journal of Physical Organic Chemistry* **2009**, *22* (5), 449–454. <https://doi.org/10.1002/poc.1489>.

- (50) Gardner, G. B.; Chen, R. F.; Berry, A. High-Resolution Measurements of Chromophoric Dissolved Organic Matter (CDOM) in the Neponset River Estuary, Boston Harbor, MA. *Marine Chemistry* **2005**, 96 (1), 137–154. <https://doi.org/10.1016/j.marchem.2004.12.006>.
- (51) Lorenzo-Seva, U.; ten Berge, J. M. F. Tucker's Congruence Coefficient as a Meaningful Index of Factor Similarity. *Methodology: European Journal of Research Methods for the Behavioral and Social Sciences* **2006**, 2 (2), 57–64. <https://doi.org/10.1027/1614-2241.2.2.57>.
- (52) Murphy, S. F. *Comprehensive Water Quality of the Boulder Creek Watershed, Colorado, during High-Flow and Low-Flow Conditions, 2000*; Water-Resources Investigations Report; USGS Numbered Series 03–4045; U.S. Geological Survey: Reston, VA, 2003; Vol. 03–4045. <https://doi.org/10.3133/wri034045>.
- (53) Kaushal, S. S.; Lewis, W. M. Patterns in the Chemical Fractionation of Organic Nitrogen in Rocky Mountain Streams. *Ecosystems* **2003**, 6 (5), 483–492.
- (54) McKnight, D. M.; Boyer, E. W.; Westerhoff, P. K.; Doran, P. T.; Kulbe, T.; Andersen, D. T. Spectrofluorometric Characterization of Dissolved Organic Matter for Indication of Precursor Organic Material and Aromaticity. *Limnology and Oceanography* **2001**, 46 (1), 38–48. <https://doi.org/10.4319/lo.2001.46.1.0038>.
- (55) Stedmon, C. A.; Markager, S.; Bro, R. Tracing Dissolved Organic Matter in Aquatic Environments Using a New Approach to Fluorescence Spectroscopy. *Marine Chemistry* **2003**, 82 (3), 239–254. [https://doi.org/10.1016/S0304-4203\(03\)00072-0](https://doi.org/10.1016/S0304-4203(03)00072-0).
- (56) Aiken, G. Fluorescence and Dissolved Organic Matter: A Chemist's Perspective. In *Aquatic Organic Matter Fluorescence*; Baker, A., Reynolds, D. M., Lead, J., Coble, P. G., Spencer, R. G. M., Eds.; Cambridge Environmental Chemistry Series; Cambridge University Press: Cambridge, 2014; pp 35–74. <https://doi.org/10.1017/CBO9781139045452.005>.
- (57) Reynolds, D. M. Rapid and Direct Determination of Tryptophan in Water Using Synchronous Fluorescence Spectroscopy. *Water Research* **2003**, 37 (13), 3055–3060. [https://doi.org/10.1016/S0043-1354\(03\)00153-2](https://doi.org/10.1016/S0043-1354(03)00153-2).
- (58) Maie, N.; Scully, N. M.; Pisani, O.; Jaffé, R. Composition of a Protein-like Fluorophore of Dissolved Organic Matter in Coastal Wetland and Estuarine Ecosystems. *Water Research* **2007**, 41 (3), 563–570. <https://doi.org/10.1016/j.watres.2006.11.006>.
- (59) Stubbins, A.; Lapierre, J.-F.; Berggren, M.; Prairie, Y. T.; Dittmar, T.; del Giorgio, P. A. What's in an EEM? Molecular Signatures Associated with Dissolved Organic Fluorescence in Boreal Canada. *Environ. Sci. Technol.* **2014**, 48 (18), 10598–10606. <https://doi.org/10.1021/es502086e>.
- (60) McKay, G. Emerging Investigator Series: Critical Review of Photophysical Models for the Optical and Photochemical Properties of Dissolved Organic Matter. *Environ. Sci.: Processes Impacts* **2020**, 22 (5), 1139–1165. <https://doi.org/10.1039/D0EM00056F>.
- (61) Leresche, F.; McKay, G.; Kurtz, T.; von Gunten, U.; Canonica, S.; Rosario-Ortiz, F. L. Effects of Ozone on the Photochemical and Photophysical Properties of Dissolved Organic Matter. *Environ. Sci. Technol.* **2019**, 53 (10), 5622–5632. <https://doi.org/10.1021/acs.est.8b06410>.
- (62) Leresche, F.; Torres-Ruiz, J. A.; Kurtz, T.; Gunten, U. von; Rosario-Ortiz, F. L. Optical Properties and Photochemical Production of Hydroxyl Radical and Singlet Oxygen after Ozonation of Dissolved Organic Matter. *Environ. Sci.: Water Res. Technol.* **2021**, 7 (2), 346–356. <https://doi.org/10.1039/D0EW00878H>.
- (63) Nöthe, T.; Fahlenkamp, H.; Sonntag, C. von. Ozonation of Wastewater: Rate of Ozone Consumption and Hydroxyl Radical Yield. *Environ. Sci. Technol.* **2009**, 43 (15), 5990–5995. <https://doi.org/10.1021/es900825f>.
- (64) Hammes, F.; Salhi, E.; Köster, O.; Kaiser, H.-P.; Egli, T.; von Gunten, U. Mechanistic and Kinetic Evaluation of Organic Disinfection By-Product and Assimilable Organic Carbon (AOC) Formation during the Ozonation of Drinking Water. *Water Research* **2006**, 40 (12), 2275–2286. <https://doi.org/10.1016/j.watres.2006.04.029>.

- (65) Tentscher, P. R.; Bourgin, M.; von Gunten, U. Ozonation of Para-Substituted Phenolic Compounds Yields p-Benzoquinones, Other Cyclic  $\alpha,\beta$ -Unsaturated Ketones, and Substituted Catechols. *Environ. Sci. Technol.* **2018**, 52 (8), 4763–4773. <https://doi.org/10.1021/acs.est.8b00011>.
- (66) Edzwald, J. K.; Becker, W. C.; Wattier, K. L. Surrogate Parameters for Monitoring Organic Matter and THM Precursors. *Journal - American Water Works Association* **1985**, 77 (4), 122–132. <https://doi.org/10.1002/j.1551-8833.1985.tb05521.x>.
- (67) Helms, J. R.; Stubbins, A.; Ritchie, J. D.; Minor, E. C.; Kieber, D. J.; Mopper, K. Absorption Spectral Slopes and Slope Ratios as Indicators of Molecular Weight, Source, and Photobleaching of Chromophoric Dissolved Organic Matter. *Limnology and Oceanography* **2008**, 53 (3), 955–969. <https://doi.org/10.4319/lo.2008.53.3.0955>.
- (68) Hansen, A. M.; Kraus, T. E. C.; Pellerin, B. A.; Fleck, J. A.; Downing, B. D.; Bergamaschi, B. A. Optical Properties of Dissolved Organic Matter (DOM): Effects of Biological and Photolytic Degradation. *Limnology and Oceanography* **2016**, 61 (3), 1015–1032. <https://doi.org/10.1002/lno.10270>.
- (69) Baker, A. Fluorescence Excitation–Emission Matrix Characterization of Some Sewage-Impacted Rivers. *Environ. Sci. Technol.* **2001**, 35 (5), 948–953. <https://doi.org/10.1021/es000177t>.
- (70) Parlanti, E. Dissolved Organic Matter Fluorescence Spectroscopy as a Tool to Estimate Biological Activity in a Coastal Zone Submitted to Anthropogenic Inputs. *Organic Geochemistry* **2000**, 17.
- (71) Huguet, A.; Vacher, L.; Relexans, S.; Saubusse, S.; Froidefond, J. M.; Parlanti, E. Properties of Fluorescent Dissolved Organic Matter in the Gironde Estuary. *Organic Geochemistry* **2009**, 40 (6), 706–719. <https://doi.org/10.1016/j.orggeochem.2009.03.002>.